Hindawi
Mathematical Problems in Engineering
Volume 2019, Article ID 4064652, 6 pages
https://doi.org/10.1155/2019/4064652

Research Article

Optimization Research on Thermal Error Compensation of FOG in Deep Mining Using Uniform Mixed-Data Design Method

Yimin Liu,[1,2] **Chenghu Wang**,[1] **Jie Wang**,[2] **and Weifeng Ji**[2,3]

[1]*Key Lab of Crustal Dynamics, Institute of Crustal Dynamics, CEA, Beijing 100085, China*
[2]*School of Manufacturing Science & Engineering, Sichuan University, Sichuan 610065, China*
[3]*The Institute of Exploration Technology of CAGS, Sichuan 611730, China*

Correspondence should be addressed to Yimin Liu; 153973418@qq.com

Received 18 October 2018; Revised 18 December 2018; Accepted 7 March 2019; Published 19 March 2019

Academic Editor: Salvatore Strano

Suffered from the unsatisfied time consumption of thermal error compensation, this paper aims to realize a faster and more accurate fibre optic gyroscope (FOG) thermal error compensation plan, so that the deep-hole inclinometer using in mining which is based on FOG will make accurate measurement under external thermal field. Using uniform mixed-data design method, it is learned that the temperature compensation experiments only consumed 1/9 the time required for traditional method within the working condition range of 0~120°C. Suffice it to say that our method can markedly enhance the efficiency of FOG temperature compensation. To this end, the finite-element method (FEM) was also applied to explore the thermal conductivity and simulate the complex boundary conditions of the FOG. Then, the Shupe error of the FOG was calculated and used to derive the FOG error compensation formula, and the factors and their levels affecting the Shupe error in thermal field were considered in error compensation experiments. After that, the optimal design of FOG thermal error compensation experiments was created by FOG error compensation formula and uniform mixed-data design table, and this plan significantly reduced the number of experiments compared to before. Finally, the design was compared with the full-scale design and orthogonal design to verify its accuracy and efficiency. The comparison shows that the proposed method can markedly enhance the efficiency of FOG error compensation and elevate the measuring accuracy of FOG. This paper innovatively applies the uniform mixed-data design method to the field of FOG measurement, and this research offers new insights into the error compensation optimization of FOG measurement.

1. Introduction

The inertial-based gyroscope is a typical application of inertia technology in the field of measurement. Recent years have seen the proliferation of the tool from high-performance space applications (e.g., planes, missiles, and satellites) to the geological mining drilling [1]. The inertial-based gyroscope can measure borehole trajectory under any formation condition, because it is immune to the interference of magnetic material, a major obstacle in geological exploration, and any other kind of external influence.

Recently, a new gyroscope, the fibre optic gyroscope (FOG), was created independent of the inertial principle. The FOG senses changes in orientation using the Sagnac effect and thus performs the function of a mechanical gyroscope. However, its principle of operation is instead based on the interference of light which has passed through a coil of optical fibre, which can be as long as 5km [2]. The main advantages of the FOG are as follows.

Firstly, a FOG provides extremely precise rotational rate information, in part because of its lack of cross-axis sensitivity to vibration, acceleration, and shock. The gyroscope no moving parts and does not rely on inertial resistance to movement. Hence, this is perhaps the most reliable alternative to the mechanical gyroscope. Second, the FOG typically shows a higher resolution than a ring laser gyroscope. Third, the FOG applies to both open-loop and closed-loop configurations.

Nevertheless, the FOG is very sensitive to the ambient temperature and suffers from a great drift and poor scale factor performance. Therefore, the measuring accuracy of FOG may be seriously affected by the variation in external temperature [3]. Under the harsh environment in super

deep boreholes, Dzhashitov et al. indicated that it is very unlikely to realize accurate heat simulation of the FOG through the traditional thermal field analysis [4]. Il'Inykh et al. solved the thermomechanics problem of how thermal loads affect the operation of a fibre optic gyroscope, and this is mainly because of the difficulty in determining the boundary scope, control equation, and thermal features of the main components [5]. Many scholars have done a lot of research work on thermal error compensation to improve FOG measuring accuracy. Zhang and Wang focused on dynamic angular velocity modeling and error compensation of one-fibre optic gyroscope in the whole temperature range, and they put forward a thermal error compensation method based on orthogonal design [6]. Sokolov et al. considered a mathematical model of a gyro stabilization system for thermal error compensation, and the stabilization system is based on fibre-optic gyroscopes (FOGs) with accelerometer correction loops [7]. Sanders et al. determined the composition of the thermal bias error of fibre-optic gyroscopes and a series of temperature experiments are designed to validate the adequacy of the selected modeling terms [8].

Due to many factors affecting the FOG, there will be an amount of experiments of thermal error compensation, and it will take a lot of experiments time. To solve this problem, this article discusses the application of finite-element method (FEM) and uniform mixed-data design. Firstly this paper explores the FOG thermal conductivity by finite-element method. The FEM was also applied to simulate the complex boundary conditions of the FOG. Then, the Shupe error of the FOG was calculated and used to derive the FOG thermal error compensation formula. After that, the optimal design of FOG error compensation experiments was innovatively created based on uniform mixed-data design. Finally, this new design was compared with the full-scale design and orthogonal design to verify its accuracy and efficiency.

2. Error Theory Analysis of FOG Thermal Field

Due to thermal field distribution and heat transfer under the thermal transient state, the physical properties, geometrical features, and thermal transfer of the FOG are dynamically changing over time, leading to Shupe error in FOG inclinometer. The Shupe error is negatively correlated with the accuracy of the inclinometer.

To enhance the accuracy, the FEM was adopted to analyse the heat conduction features of the inclinometer in thermal field. This method can overcome the limits of traditional analytical techniques. For instance, it can handle the complex boundary conditions of the FOG. According to the differential control equations of heat conduction, a FOG error compensation formula in thermal field was derived through the Shupe error analysis, laying the basis for FOG thermal field modelling and error compensation.

2.1. Shupe Error Analysis. In the thermal transient state, the Shupe error can be calculated based on the phase delay ϕ of the light wave propagation in the fibre loop with length L [9]:

$$\phi = \int_0^L \beta(z)\,dz = \int_0^L \beta_0 n(z)\,dz \tag{1}$$

where β_0 is the propagation constant of light in free space and n(z) is refractive index. Since the thermal expansion and refractive index of the medium may vary with the thermal fields during light wave propagation, (1) can be rewritten as

$$\phi = \beta_0 n_{eff} L + \beta_0 \left(\frac{\partial n_{eff}}{\partial T} + n_{eff}\alpha \right) \int_0^L \Delta T(z)\,dz \tag{2}$$

where n_{eff} is fibre refractive index; $(\partial_{neff})/\partial_T$ is the temperature coefficient; α is fibre thermal expansion coefficient; $\Delta T(z)$ is the temperature change. Using the Sagnac effect, the FOG measures the phase difference of two beams of light wave through the same optical fibre with length L. One beam of light wave propagates in the clockwise direction and the other in the opposite direction. Specifically, the clockwise phase delay $\phi_{cw}(t)$ and the counter-clockwise phase delay $\phi_{ccw}(t)$ are calculated, and the Shupe error $\Delta\phi_E(\text{Shupe})$ in the thermal transient state is given a differential time definition [10]. $\Delta\phi_E(\text{Shupe})$ can be calculated by

$$\Delta\phi_E(Shupe) = \frac{\beta_0}{c_m} \left(\frac{\partial n_{eff}}{\partial T} + n_{eff}\alpha \right) \int_0^L \dot{T}(z,t)(L-2z)\,dz \tag{3}$$

where T(z,t) is the temperature change rate in the fibre loop ($T(z,t)=\partial T/\partial z$). Equation (3) shows that the Shupe error reflects how the temperature gradient affects the FOG measuring accuracy. To sum up, the Shupe error $\Delta\phi_E(\text{Shupe})$, induced by the thermal field variation in the transient state, has a certain effect on the output light intensity I of the FOG in that it reduces the measuring accuracy of FOG inclinometer. The output light intensity I can be obtained as follows:

$$I = I_0 \{1 + \cos[\phi_S + \Delta\phi_S(Shupe)]\} \tag{4}$$

2.2. FOG Error Compensation Formula in Thermal Field. Under the joint action of Shupe error $\Delta\phi_E(\text{Shupe})$ and the additional phase shift $\phi_{\Delta L}$ in the transient state, an error will occur in the Sagnac phase shift ϕ_S. Based on the previous analysis on Shupe error, this section attempts to deduce the error formula in the thermal transient state and then the FOG error compensation formula in thermal field.

Due to the thermal field and the thermal stress in the FOG, the fibre loop length L changes by a certain degree. Hence, there is $L/d \gg 1$ with d being fibre diameter. By the definition of thermal expansion coefficient [11], the thermal expansion coefficient α of the optical fibre in the thermal transient state can be expressed as

$$\alpha = \frac{d(\Delta z)}{\Delta z \cdot d[T(z,t)]} \tag{5}$$

where z is a point on the optical fibre loop of the FOG in (5). Then, the linear deformation of the fibre loop ΔL leads to a Sagnac equivalent phase shift $\phi_{\Delta L}$:

$$\phi_{\Delta L} = \Delta L \cdot \frac{\partial \phi_S}{\partial L} = \Delta T \cdot \alpha \cdot L \cdot \frac{\partial \phi_S}{\partial L} \tag{6}$$

$$\Delta\phi_S(\Delta L) = \alpha \cdot \frac{\partial \phi_S}{\partial L} \cdot \sum \Delta T(z,t) \cdot \Delta z \tag{7}$$

Table 1: The table of experimental factors and their levels.

Factor	Level	Unit	Value
Temperature range	6	˚C	0~70; 10~80; 20~90;30~100; 40~110; 50~120
Angular velocity	12	˚/s	0; ±2.5; ±5; ±10; ±20; ±40; 80
Effective refractive index	4	/	1.4770; 1.4719; 1.4685; 1.4680
Temperature change rate	4	˚C/min	0.5; 1; 2; 4

It can be seen that $\Delta\phi_S$(Shupe) in the thermal transient state is correlated with the linear expansion coefficient α and effective refractive index n_{eff} of the optical fibre: $\Delta\phi_S(\text{Shupe}) = F(\alpha) = (\alpha, \ldots, n_{eff})$. Then, (8) and (9) are derived by finding the partial derivatives of α and n_{eff}, and (8) and (9), respectively, depict the effect of Sagnac phase shift in thermal transient state caused by the linear deformation and refractive index variation of the optical fibre, and the linear expansion coefficient α is determined by the material of the fibre.

$$\frac{\partial\left[\Delta\phi_S\left(Shupe\right)\right]}{\partial\alpha} = \frac{\beta_0}{c_m}\cdot n_{eff}\cdot\int_0^L \dot{T}\left(z,t\right)\left(L-2z\right)dz \tag{8}$$

$$\frac{\partial\left[\Delta\phi_S\left(Shupe\right)\right]}{\partial\alpha} = \left(\frac{\alpha\beta_0}{c_m} + \frac{\partial\left(\partial n_{eff}/\partial T\right)}{\partial n_{eff}}\right)\int_0^L \dot{T}\left(z,t\right)\left(L-2z\right)dz \tag{9}$$

On the premise of using the same material fibre and combined with (3), (8), and (9), error theory analysis shows that the factors affecting the Shupe error of FOG in thermal field are mainly the temperature change rate, the effective refractive index, and the angular velocity. For these different impact factors and their levels, in the next chapter the error compensation experiments with different influence factors and their levels have been designed to improve the measurement accuracy of FOG, so these formulas serve as the guide for FOG error compensation in thermal field, paving the effective way for a rational error compensation plan.

3. Error Compensation Optimizations Based on Uniform Mixed Data Design

3.1. FOG Dynamic Error Model. The measuring errors of the FOG are mostly nonlinear [12]. However, it is immensely difficult to create an accurate nonlinear error model. With the existing static error models, the error compensation effect has been far from desirable. Fortunately, the FOG dynamic error model is an ideal way to solve the problem. The model depicts the mathematical relationship between measuring error and angular velocity (angular acceleration) of the gyroscope in angular motion [13]. The expression of the model is as follows:

$$\begin{aligned} E_{\boldsymbol{\omega}} = {} & D_0 + D_1\dot{\boldsymbol{\omega}}_x + D_2\dot{\boldsymbol{\omega}}_y + D_3\dot{\boldsymbol{\omega}}_z + D_4\boldsymbol{\omega}_x + D_5\boldsymbol{\omega}_y \\ & + D_6\boldsymbol{\omega}_z + D_7\boldsymbol{\omega}_x^2 + D_8\boldsymbol{\omega}_y^2 + D_9\boldsymbol{\omega}_z^2 + D_{10}\boldsymbol{\omega}_x\boldsymbol{\omega}_y \\ & + D_{11}\boldsymbol{\omega}_y\boldsymbol{\omega}_z + D_{12}\boldsymbol{\omega}_x\boldsymbol{\omega}_z \end{aligned} \tag{10}$$

where ω_x, ω_y, ω_z, $\dot{\omega}_x$, $\dot{\omega}_y$, and $\dot{\omega}_z$ are, respectively, the angular velocity (angular acceleration) of the sensor relative to the inertial conductor along different axes; E_ω is the value error of the dynamic model; D_0 is the dynamic constant; $D_1 \sim D_{12}$ are the error coefficients corresponding to the relative angular velocities (angular accelerations). The error coefficients can be obtained by error compensation experiments, and the FOG dynamic error model is about the determination of the above coefficients and parameters determination [14].

3.2. Error Compensation Based on Uniform Mixed-Data Design. The determination of coefficients and parameters in FOG error compensation requires a massive amount of data based on triaxial quadrature calibration bench and a series of calibration instruments [15]. The thermal modelling is often adopted to compensate the FOG output, aiming to reduce the effect of thermal change on output accuracy.

As mentioned in the previous section, the factors affecting the FOG measurement accuracy in this experiment are the temperature change rate, the effective refractive index, and the angular velocity. Due to the higher temperature in deep mining hole, up to 250˚C, a metal vacuum flask has been designed to ensure that its internal space does not exceed 125˚C degrees [16] and the temperature range of measuring chip is set from 0˚C to 120˚C.

Therefore, there are four influence factors in the FOG error compensation experiments, namely, experimental temperature range, temperature change rate, effective refractive index, and angular velocity, which employed a four-layer network structure. The parameter values (number of levels) of each factor are shown in Table 1.

The thermal error compensation experiments usually employ a network structure of three to four layers [17]. Both full-scale design experiment and orthogonal experiment are time-consuming and low in FOG error compensation efficiency. Therefore, the mixed-data design is introduced to the FOG error compensation in this research. In addition to high uniformity and sound accuracy, the mixed-data design is known for its ability of error compensation with a few numbers of experiments. It is an ideal option for FOG error compensation experiments.

Table 2 presents a recommended uniform mixed-data design. The design boasts good uniformity and comprehensiveness and avoids repeated experiments. Table 1 can be shown as the uniform mixed-data table U_{12} $(12*6*4^2)$, through the combination of column1, column2, column3, and column4; it can be obtained through the following [18]:

$$D\left(x_1,\cdots,x_n\right) = \sup_{x\in c^m}\left|\frac{n_x}{n} - v\left(x\right)\right| \tag{11}$$

(a) (b)

Figure 1: (a) Photo of the FOG error compensation experiments on the triaxial quadrature calibration bench and (b) photo of the FOG error compensation experiments in thermostat.

Table 2: $U_{12}(12*6*4^2)$.

No.	1	2	3	4
1	1	2	2	4
2	2	3	3	4
3	3	5	4	4
4	4	6	1	3
5	5	1	3	3
6	6	3	4	3
7	7	4	1	2
8	8	6	2	2
9	9	1	4	2
10	10	2	1	1
11	11	4	2	1
12	12	5	3	1
D		0.3274		

where $x_1, \ldots, x_n$ are n homogeneously dispersed points in $U_{12}(12*6*4^2)$; $x=(x_1, \ldots, x_m) \in C_m$ is a vector in the matrix; $v(x)= x_1, \ldots, x_m$ is the volume of the rectangle [0, x]; $n_x \in (x_1, \ldots\ldots, x_n)$ is the number of points falling in [0, x]; n_x/n is the percentage of points falling in the rectangle [0,x] [19]. The deviation of $U_{12}(12*6*4^2)$ from formula D is 0.3274.

4. Experimental Results and Discussion

The table of FOG error compensation experiments was designed by uniform mixed-data design. Then, the factors and their levels reference Table 1 and the test elements are placed to the corresponding position according to Table 2. The resultant table is displayed in Table 3, and A represents the angular velocity, B represents the temperature range, C represents the temperature change rate, and D represents the effective refractive index.

Taking the data of the 9th experiment (Table 2), for example, the effective refractive index is 1.4719, and the angular velocity is set to 10°/s and the temperature of the thermostat was initialized as 0°C. Then, the temperature is increased to 70°C at the heating rate of 4°C/min. After that, the FOG output data are collected at an interval of 1 second for thermal error compensation. Next, the temperature is decreased to 0°C at the cooling rate of -4°C/min. The 9th experiment lasted about 35min after calculation. The time consumption of the other experiments is measured similarly and recorded in Table 4, and then this plan adds the time of each group to get the total time of the error compensation experiments.

According to Table 3, the error compensation experiments (temperature range: 0°C~120°C) consume a total of 26.5 hours. If the full-scale design experiment was adopted, the time consumption at each point would be 20 hours, putting the total duration at 240 hours. This means the uniform mixed-data design experiments only consume 1/9 the time required for a full-scale design experiment. The four factors in the error compensation plan each have 12, 6, 4, and 4 levels. Hence, there would be 1,152 different combinations for orthogonal experiments. In comparison, the number of uniform mixed-data designs is only 12. It is clear that the uniform mixed-data design experiments could achieve similar results with the orthogonal experiments through much fewer experiments.

Figures 1(a) and 1(b) are two photos of the FOG error compensation experiments on the triaxial quadrature calibration bench.

Then, the angular velocity was kept constant to reveal the effect of temperature range, heating rate, and cooling rate. To validate the accuracy, the experimental data of the uniform mixed-data design method was compared with those of a full-scale design experiment. Two curves on thermal error compensation value (measuring accuracy) were drawn for each method (see Figure 2).

As shown in Figure 2, the uniform mixed-data design had a similar error compensation effect to that of fully-scale design, when the angular velocity was kept constant. The two curves were well fitted, with the maximum absolute error of 0.068°. The results show that the uniform mixed-data design has a fairly good accuracy and fulfills the accuracy demand of FOG measurement.

5. Conclusions

Authors should discuss the results and how they can be interpreted in perspective of previous studies and of the working hypotheses. The findings and their implications

Table 3: Uniform mixed-data design table of experiments.

No.(n)	A(°/s)	B(°C)	C(°C/min)	D
1	-40	10~80	1	1.4680
2	-20	20~90	2	1.4680
3	-10	40~110	4	1.4680
4	-5	50~120	0.5	1.4685
5	-2.5	0~70	2	1.4685
6	0	20~90	4	1.4685
7	2.5	30~100	0.5	1.4719
8	5	50~120	1	1.4719
9	10	0~70	4	1.4719
10	20	10~80	0.5	1.4770
11	40	30~100	1	1.4770
12	80	40~110	2	1.4770
D		0.3274		

Table 4: Time consumption of the error compensation experiments.

No.	1	2	3	4	5	6	7	8	9	10	11	12
Rate(°/s)	-40	-20	-10	-5	-2.5	0	2.5	5	10	20	40	80
Time consumption (min)	140	70	35	280	70	35	280	140	35	280	140	70

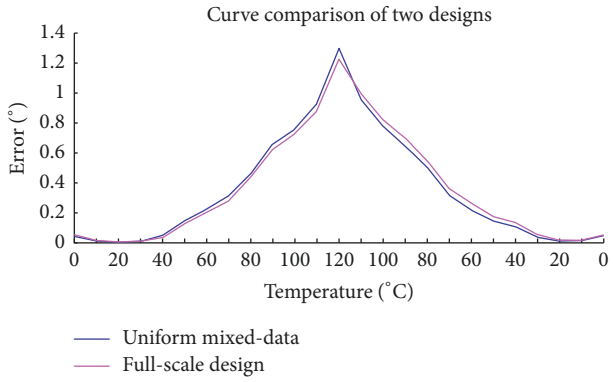

Figure 2: Effect of uniform mixed-data design and full-scale design.

should be discussed in the broadest context possible. Future research directions may also be highlighted.

Under the external thermal field in deep-hole mining, the FOG suffers from a great drift and poor scale factor performance. The drift would seriously affect the measuring accuracy of the FOG inclinometer. The full-scale design experimental plan or orthogonal experimental plan was previously used for thermal error compensation. Because of many factors such as temperature changing rate, rotational speed of FOG, and temperature range, which will seriously affect accuracy of FOG in thermal field, there will be an amount of error compensation experiments. Suffered from the unsatisfied time consumption, previous plan were unsuitable for thermal error compensation. Thus, it is necessary to pursue fast and accurate FOG temperature compensation and high measuring accuracy. For this purpose, this paper puts forward the following new optimization measures based on the FEM and uniform mixed-data design. The advantages of this plan are as follows:

(1) The Shupe error, induced by external thermal field, was calculated by heat transfer theory and FEM of heat conduction. On this basis, the thermally induced equivalent phase shift and thermally induced errors of the FOG were deduced. Then, the FOG error compensation formulas were derived, laying the basis for FOG error compensation plan, and the FOG error compensation formulas significantly improve accuracy of thermal error compensation.

(2) The uniform mixed-data design was applied to optimize the experiments on FOG temperature compensation model. Here, a uniform mixed-data design is presented considering the effect of angular velocity and temperature. First, a uniform mixed-data table was set up by the mixture-data uniform design method; then, the optimal experimental plan was prepared in light of the table. Through comparison, it is learned that the uniform mixed-data design experiments only consumed 1/9 the time required for a full-scale design experiment and significantly reduced the number of experiments.

This paper innovatively applies the uniform mixed-data design method to the field of FOG measurement, and suffice it to say that our method can markedly enhance the efficiency of FOG thermal error compensation and elevate the measuring accuracy of FOG, and it will be a great significance to expand engineering application of FOG.

Data Availability

No data were used to support this study.

Conflicts of Interest

The authors declare that there are no conflicts of interest regarding the publication of this paper.

Acknowledgments

This research was funded by National Key Scientific Instrument and Equipment Development Project of China, grant number 2013YQ050791, by National Natural Science Youth Foundation of China, grant number 41804089, by Project of Observation Instrument Development for Integrated Geophysical Field of China Mainland, grant number Y201802, and by National Natural Science Foundation of China, grant number 41574088.

References

[1] A. Lawrence, *Modern Inertial Technology. Navigation, Guidance, and Control*, Springer, New York, NY, USA, 1993.

[2] J. M. López-Higuer, *Handbook of Fibre Optic Sensing Technology*, John Wiley & Sons, Hoboken, NJ, USA, 2000.

[3] M. Tuckness, "Error analysis for a navigation algorithm based on optical-flow and a digital terrain map," in *Proceedings of the IEEE Conference on Computer Vision Pattern Recognition*, pp. 604–610, 2004.

[4] V. E. Dzhashitov and V. M. Pankratov, "The determined chaos in disturbed by temperature dynamic systems with gyros," in *Proceedings of the IEEE International Conference on Physics Control*, pp. 638–643, 2003.

[5] O. Y. Smetannikov and G. V. Il'Inykh, "Study of the thermomechanical behavior of the interface module of a fiber-optic gyroscope," *Journal of Optical Technology (A Translation of Opticheskii Zhurnal)*, vol. 81, no. 7, pp. 397–402, 2014.

[6] Y.-S. Zhang, Y. Y. Wang, T. Yang, R. Yin, and J. C. Fang, "Dynamic angular velocity modeling and error compensation of one-fiber fiber optic gyroscope (OFFOG) in the whole temperature range," *Measurement Science and Technology*, vol. 23, no. 2, Article ID 025101, 2012.

[7] A. V. Sokolov, A. A. Krasnov, L. P. Starosel'tsev, and A. N. Dzyuba, "Development of a gyro stabilization system with fiber-optic gyroscopes for an air-sea gravimeter," *Gyroscopy and Navigation*, vol. 6, no. 4, pp. 338–343, 2015.

[8] F. Mohr and F. Schadt, "Bias error in fiber optic gyroscopes due to elastooptic interactions in the sensor fiber," in *Proceedings of the Second European Workshop on Optical Fibre Sensors, EWOFS'04*, pp. 410–413, Spain, June 2004.

[9] F. Mohr, "Thermooptically induced bias drift in fiber optical sagnac interferometers," *Journal of Lightwave Technology*, vol. 14, no. 1, pp. 27–41, 1996.

[10] M. Raab and T. Quast, "Two-color Brillouin ring laser gyro with gyro-compassing capability," *Optics Expresss*, vol. 19, no. 18, pp. 1492–1494, 1994.

[11] S. Haykin Simon, *Neural Networks and Learning Machines*, Prentice Hall, New York, NY, USA, 2008.

[12] T. Tavio and A. Tata, "Predicting Nonlinear behavior ad stress-strain relationship of rectangular confined reinforced concrete columns with ANSYS," *Civil Engineering Dimension*, vol. 11, no. 1, pp. 23–31, 2009.

[13] M. Biel, C. Wahl-Schott, S. Michalakis, and X. Zong, "Integration of GIS and artificial neural network for prediction of ozone concentration in semirural areas of Rawalpindi and Islamabad," *Physiological Reviews*, vol. 89, no. 3, pp. 847–885, 2009.

[14] J. M. L and J. M. López-Higuer, *Handbook of Fibre Optic Sensing Technology*, John Wiley & Sons, Hoboken, NJ, USA, 2000.

[15] O. Cazacu, N. Chandola, J. L. Alves, and B. Revil-Baudard, "Importance of the consideration of the specificities of local plastic deformation on the response of porous solids with Tresca matrix," *European Journal of Mechanics - A/Solids*, vol. 47, pp. 194–205, 2014.

[16] Y. Liu, J. Wang, W. Ji, and G. Luo, "Temperature field finite element analysis of the ultra-high temperature borehole inclinometer based on FOG and its optimization design," *Chemical Engineering Transactions*, vol. 51, pp. 709–714, 2016.

[17] Y. Meng, Y. Chen, S. Li et al., "Research on the orthogonal experiment of numeric simulation of macromolecule-cleaning element for sugarcane harvester," *Materials and Corrosion*, vol. 30, no. 6, pp. 2250–2258, 2009.

[18] N. I. Muskhelishvili, "Some basic problems of the mathematical theory of elasticity," *Civil Engineering Dimension*, vol. 15, no. 5, pp. 445–447, 2009.

[19] G. Vasudevan, S. Kothandaraman, and S. Azhagarsamy, "Study on non-linear flexural behavior of reinforced concrete beams using ANSYS by discrete reinforcement modeling," *International Journal of Strength of Materials*, vol. 45, no. 2, pp. 231–241, 2013.